Denoising of the Speckle Noise by Robust Low-rank Tensor Decomposition

Calis, Metin; Hunyadi, Borbála

DOI
10.23919/EUSIPCO63174.2024.10715120

Publication date
2024

Document Version
Final published version

Published in
32nd European Signal Processing Conference, EUSIPCO 2024 - Proceedings

Citation (APA)
Calis, M., & Hunyadi, B. (2024). Denoising of the Speckle Noise by Robust Low-rank Tensor Decomposition. In *32nd European Signal Processing Conference, EUSIPCO 2024 - Proceedings* (pp. 1157-1161). (European Signal Processing Conference). European Signal Processing Conference, EUSIPCO. https://doi.org/10.23919/EUSIPCO63174.2024.10715120

Denoising of the Speckle Noise by Robust Low-rank Tensor Decomposition

Metin Calis
Department of Microelectronics
Delft University of Technology
Delft, Netherlands
m.calis@tudelft.nl

Borbála Hunyadi
Department of Microelectronics
Delft University of Technology
Delft, Netherlands
b.hunyadi@@tudelft.nl

***Abstract*—Speckle noise is commonly assumed to be multiplicative. Non-local speckle denoising algorithms stack the correlated data patches into a tensor and take the logarithm such that the noise becomes additive. The log-transformed speckle noise is commonly assumed to be white Gaussian noise. The denoising is done through the low-rank approximation techniques applied to the non-local data patches. However, the log-transformed speckle noise can be better approximated as white Gaussian noise with sparse outliers. In this paper, we model the log-transformed speckle noise with this assumption and assess the importance of the noise model under various SNRs. In addition, we propose a weighting scheme for the tensor-based low-rank convex denoising method that utilizes the known ranks. The performance of the proposed algorithm is benchmarked against truncated multilinear singular value decomposition, higher-order orthogonal iteration, and robust tensor decomposition methods that use the sum of the nuclear norm and the tubal nuclear norm. Robust tensor decomposition methods that use the tubal nuclear norm perform better in low SNR scenarios. For high SNR scenarios, the proposed algorithm is found to perform better.**

***Index Terms*—speckle denoising, low-rank approximation, outlier resistant, convex optimization, tensor decomposition**

I. INTRODUCTION

Speckle noise is an inherent characteristic of coherent imaging modalities occurring in various systems, including synthetic aperture radar [1], sonar [2], and ultrasound imaging [3]. This phenomenon arises due to the superposition of waves reflected from a resolution cell, which is defined by the bandwidth of the transmitted signal. When enough scatterers have sizes comparable to the transmitted signal's wavelength and the system's point spread function is broader, the received signal exhibits a granular appearance. Speckle noise is commonly reduced to enhance the visibility of structures and improve the quantification of the underlying system's dynamics.

In many applications, speckle noise is assumed to be multiplicative [1] [2] [3]. Several techniques were proposed in the literature to remove multiplicative noise. State-of-the-art methods can be categorized as the total variation (TV) regularization [4] [5], and nonlocal low-rank-based methods [2] [6]. Total regularization methods optimize a loss function that includes a data fidelity term and a total variational term. The data fidelity term provides a least squares approximation, while the total variation regularization term smoothes the data while preserving the edges. The nonlocal low-rank-based methods first cluster the data into similar patches and apply denoising by returning a low-rank approximation of each patch. This low-rank approximation is made through algorithms such as higher-order orthogonal iteration (HOOI) [2] or a convex relaxation of the low rankness [7]. However, these algorithms are better suited for white Gaussian noise (WGN). The aforementioned techniques can be improved by changing the WGN assumption about the speckle noise.

In [3], the log-transformed Rayleigh distribution is approximated as WGN with sparse outliers. The sparse outliers have a detrimental effect on the low-rank approximation of the data [8]. The robust tensor decomposition methods recover the low-rank tensor while capturing noise as a sparse and additive term. In most algorithms, the sparsity constraint is relaxed using the L_1 norm. The convex relaxation of the tensor low rankness differs and can be categorized into the sum of the nuclear norm-based (SNN) and the sum of tubal nuclear norm-based (TNN) methods. In [9], an SNN method is used as a robust tensor decomposition method. Assuming that the tensor is not simultaneously low-ranked in all modes, the authors in [10] introduced a new low-rank relaxation that is better suitable.

The authors in [11] introduced TNN as a tighter convex surrogate for tensor low rankness. Using TNN, the authors in [12] solved the robust tensor decomposition problem. In [13], the authors extended the TNN to consider low rankness in all modes simultaneously and introduced an orientation invariant tubal nuclear norm (OITNN-O) method. If the tensor is not low-ranked in all modes, a method named OITNN-L is introduced. TNN-based algorithms are shown to perform better than their SNN counterparts. This paper reviews SNN and TNN-based robust tensor decomposition methods and applies them in the context of speckle denoising. In addition, we propose a weighting scheme for SNN when the underlying ranks are known. In parallel with the truncated multilinear singular value decomposition (tr-MLSVD), the proposed algorithm preserves the predominant singular values while subjecting the remaining ones to soft thresholding. By incorporating a sparsity constraint, our objective is to examine the effect of sparsity in denoising speckle noise.

In Section II, we explain the notation. In Section III, we formulate the problem. In Section IV, we introduce the proposed algorithm. In Section VI and Section VII, we compare the performance of the proposed algorithm to other methods in the literature and report the results. Finally, in Section VIII, we discuss the results and propose possible future work.

II. Notation and Tensor Preliminaries

Tensors are represented by underlined boldface letters such as $\underline{\mathbf{Y}}$. Matrices are represented by boldface letters such as $\mathbf{I}$. The numbers given as superscripts in parentheses refer to the different matrices or tensors that share a similar property. An example could be the relation $\underline{\mathbf{K}} = \sum_i \underline{\mathbf{K}}^{(i)}$ for $i \in \{1, ..., N\}$. Vectors are represented with boldface lowercase letters such as $\mathbf{t}_{ij}$ that represent the (i, j)th vector of $\mathbf{T} \in \mathbb{R}^{I \times J \times K}$. Scalars are represented by lower case letters such as a_{ij} that represent element at the ith row and jth column of $\mathbf{A} \in \mathbb{R}^{I \times J}$. The fibers are the vectors extracted from the third dimension of a 3-dimensional tensor. The mode-n unfolding of $\underline{\mathbf{Y}} \in \mathbb{R}^{I_1 \times I_2 \times \cdots \times I_N}$ is $\mathbf{Y}_{(n)} \in \mathbb{R}^{I_n \times I_1 I_2 \ldots I_{n-1} I_{n+1} \ldots I_N}$. Mode-$(n, n+1)$ unfolding of a tensor is described further in the paper and shown with $\underline{\mathbf{Y}}_{[n]} \in \mathbb{R}^{I_n \times D/(I_n I_{n+1}) \times I_{n+1}}$, where $D = \prod_i I_i$. The Hadamard product is shown with $\odot$. The circular convolution is shown with $\circledast$. The Frobenius norm is the square root of the sum of each element and is shown by $|| \cdot ||_F$. The cardinality, defined as the number of non-zero elements, is shown with $|| \cdot ||_0$. The nuclear norm is shown with $|| \cdot ||_*$. The penalty parameter of augmented lagrangian is defined as ρ.

III. Problem Formulation

Let $\underline{\tilde{\mathbf{Y}}} \in \mathrm{R}^{I_1 \times I_2 \times \cdots \times I_N}$ denote the N-dimensional tensor to be denoised. We model the tensor $\underline{\tilde{\mathbf{Y}}}$ as the element-wise multiplication of the low-rank tensor $\underline{\tilde{\mathbf{L}}}$ and the noise tensor $\underline{\tilde{\mathbf{M}}}$, that is,

$$\underline{\tilde{\mathbf{Y}}} = \underline{\tilde{\mathbf{L}}} \odot \underline{\tilde{\mathbf{M}}} , \tag{1}$$

where each element of $\underline{\tilde{\mathbf{M}}}$ is modeled by the Rayleigh noise with a scaling parameter of 1. Taking the element-wise logarithm of (1) transforms the multiplicative noise into additive noise. Let the logarithms $\log \underline{\tilde{\mathbf{Y}}}$, $\log \underline{\tilde{\mathbf{L}}}$ and $\log \underline{\tilde{\mathbf{M}}}$ be denoted with $\underline{\mathbf{Y}}$, $\underline{\mathbf{L}}$ and $\underline{\mathbf{M}}$, respectively. Each element of $\underline{\mathbf{M}}$ follows the Fisher-tippet distribution.

In [3], using Taylor expansion, the Fisher-tippet distribution is approximated as WGN with sparse outliers. With these assumptions, we can model the received tensor $\underline{\mathbf{Y}}$ as the sum of a low-rank tensor $\underline{\mathbf{L}}$, sparse outlier $\underline{\mathbf{S}}$ and WGN $\underline{\mathbf{W}}$, that is,

$$\begin{aligned} \log(\underline{\tilde{\mathbf{Y}}}) &= \log(\underline{\tilde{\mathbf{L}}}) + \log(\underline{\tilde{\mathbf{M}}}) , \\ \underline{\mathbf{Y}} &= \underline{\mathbf{L}} + \underline{\mathbf{M}} , \\ \underline{\mathbf{Y}} &\approx \underline{\mathbf{L}} + \underline{\mathbf{S}} + \underline{\mathbf{W}} . \end{aligned} \tag{2}$$

This paper uses tensor approaches to compare convex methods to recover $\underline{\mathbf{L}}$ from the speckled $\underline{\mathbf{Y}}$. For $N > 2$, and ranks $r_i < I_i$ for $i \in \{1, ..., N\}$, this problem can be formulated as

$$\begin{aligned} \min_{\underline{\mathbf{L}}, \underline{\mathbf{S}}} & \left\{ \frac{1}{2} || \underline{\mathbf{L}} + \underline{\mathbf{S}} - \underline{\mathbf{Y}} ||_F^2 + \lambda || \underline{\mathbf{S}} ||_0 \right\} \\ \text{s.t.} \quad & \operatorname{rank}(\mathbf{L}_{(i)}) = r_i . \end{aligned} \tag{3}$$

The objective function given at (3) is not convex. A common convex relaxation of the cardinality is the L_1 norm. For the convex relaxation of the tensor low-rankness, we investigate two approaches, namely SNN and TNN. In the following section, we will introduce SNN and TNN. In addition, we will introduce a weighted SNN proximity operator, which can be used if the multilinear ranks of the low-rank tensor are known. We aim to apply various convex relaxations to solve (3) and compare the results in the context of speckle denoising for various SNRs, which has not been done before.

IV. Sum of Nuclear Norm (SNN)

The sum of the nuclear norm is a direct extension of the matrix rank to the tensor rank using the Tucker rank, i.e., the rank of the different unfolding of the tensor. In [9], the optimization problem given at (3) is solved through the relaxation of the low rankness using the sum of the nuclear norm. We have the following optimization problem defined as

$$\min_{\underline{\mathbf{L}}, \underline{\mathbf{S}}} \left\{ \frac{1}{2} || \underline{\mathbf{L}} + \underline{\mathbf{S}} - \underline{\mathbf{Y}} ||_F^2 + \gamma_L \sum_{i=1}^{N} || \mathbf{L}_{(i)} ||_* + \gamma_S || \underline{\mathbf{S}} ||_1 \right\} . \tag{4}$$

This can be solved by following [9], where N auxiliary variables are defined to separate $\mathbf{L}_{(i)}$ for $i \in \{1, ..., N\}$ and a proximity operator is employed alternately. The proximity operators are commonly used to minimize a function involving norms. The proximity operator of the nuclear norm is defined as

$$\operatorname{prox}_{\gamma_L/\rho}^{||\cdot||_*}(\mathbf{L}_{(i)}) = \mathbf{U} \, \mathbf{D}_{\gamma_L/\rho} \, \mathbf{V}^T , \tag{5}$$

with SVD of $\mathbf{L}_{(i)} \in \mathrm{R}^{I_i \times \prod_{n \neq i} I_n}$ defined as $\mathbf{L}_{(i)} = \mathbf{U} \, \mathbf{D} \, \mathbf{V}^T$ and $\mathbf{D}_{\gamma_L/\rho} = \max\{\mathbf{D} - \mathbf{I} \, \gamma_L/\rho, \mathbf{0}\}$.

A. Weighted Sum of Nuclear Norm

We propose a weighting scheme for SNN methods that utilizes the known multilinear ranks of the true tensor. It is suggested in [14] that the proximity operator given at (5) is problematic for denoising. This is due to the global soft thresholding operator applied to all the singular values. A better algorithm for denoising tasks can be arranged by the weighted sum of the singular value. The problem is still convex with this additional update. The highest eigenvalues corresponding to the signal subspace would be kept the same at each optimization iteration, while the lowest eigenvalues corresponding to the noise subspace would be reduced by γ_L/ρ. For the ith mode unfolding with the corresponding rank r_i, the weighted thresholding matrix $\tilde{\mathbf{D}}_{\gamma_L/\rho}$ becomes

$$\tilde{\mathbf{D}}_{\gamma_L/\rho} = \max\{\mathbf{D} - \mathbf{C}^{(i)} \, \gamma_L/\rho, \mathbf{0}\} , \tag{6}$$

where

$$\mathbf{C}^{(i)} = \begin{bmatrix} \mathbf{0} \in \mathrm{R}^{r_i \times r_i} & \mathbf{0} \in \mathrm{R}^{r_i \times I_i - r_i} \\ \mathbf{0} \in \mathrm{R}^{I_i - r_i \times r_i} & \mathbf{I} \in \mathrm{R}^{I_i - r_i \times I_i - r_i} \end{bmatrix} , \tag{7}$$

and $i \in \{1, ..., N\}$. Hence, the proximity operator defined at (5) becomes

$$\operatorname{prox}_{\gamma/\rho}^{||\cdot||_*}(\mathbf{L}^{(i)}) = \mathbf{U} \, \tilde{\mathbf{D}}_{\gamma/\rho} \, \mathbf{V}^T . \tag{8}$$

The problem at (4) can be solved the same as [9] only by changing the proximity operator from (5) to (8). We name this method weighted SNN (wSNN).

V. Tubal Nuclear Norm (TNN)

The tubal nuclear norm is introduced using the framework of t-SVD [15]. Here, we will describe the basics of the framework.

Definition 1. The t-product: Given two 3D tensors $\underline{\mathbf{T}}^{(1)} \in \mathbb{R}^{I_1 \times I_2 \times I_3}$ and $\underline{\mathbf{T}}^{(2)} \in \mathbb{R}^{I_2 \times I_4 \times I_3}$, the t-product $\underline{\mathbf{T}} = \underline{\mathbf{T}}^{(1)} * \underline{\mathbf{T}}^{(2)} \in \mathbb{R}^{I_1 \times I_4 \times I_3}$ is computed by $\mathbf{t}_{i_1 i_4} = \sum_{i_2=1}^{I_2} \mathbf{t}^{(1)}_{i_1 i_2} \circledast \mathbf{t}^{(2)}_{i_2 i_4}$.

Definition 2. The transpose: The transpose of tensor $\underline{\mathbf{T}} \in \mathbb{R}^{I_1 \times I_2 \times I_3}$ is defined as the tensor $\underline{\mathbf{T}}^T \in \mathbb{R}^{I_2 \times I_1 \times I_3}$.

Definition 3. t-SVD: The t-SVD of the tensor $\underline{\mathbf{T}} \in \mathbb{R}^{I_1 \times I_2 \times I_3}$ is defined as $\underline{\mathbf{T}} = \underline{\mathbf{U}} * \underline{\boldsymbol{\lambda}} * \underline{\mathbf{V}}^T$ with orthogonal $\underline{\mathbf{U}} \in \mathbb{R}^{I_1 \times I_1 \times I_3}$ and $\underline{\mathbf{V}} \in \mathbb{R}^{I_2 \times I_2 \times I_3}$, and $\underline{\boldsymbol{\lambda}} \in \mathbb{R}^{I_1 \times I_2 \times I_3}$ has diagonal frontal slices. The orthogonality is defined as $\underline{\mathbf{U}} * \underline{\mathbf{U}}^T = \underline{\mathbf{U}}^T * \underline{\mathbf{U}} = \underline{\mathbf{I}} \in \mathbb{R}^{I_1 \times I_1 \times I_3}$ and the identity tensor is a tensor whose first frontal slice is an identity matrix and the rest of the slices are zero matrices. The number of non-zero fibers in tensor $\underline{\boldsymbol{\lambda}}$ is called the tubal rank.

Definition 4. Mode (k,t) unfolding: $\underline{\mathbf{T}} \in \mathbb{R}^{I_1 \times \cdots \times I_N}$, the mode (k,t) unfolding creates a 3D tensor of size $\underline{\mathbf{T}}_{(k,t)} \in \mathbb{R}^{I_k \times D/I_k I_t \times I_t}$ by permuting the kth dimension of $\underline{\mathbf{T}}$ to the first, t-th dimension to the last and grouping the rest. Here D is defined as $\prod_i I_i$. Orientation invariant tubular nuclear norm is defined commonly by traversing $k \in \{1, ..., N\}$ and fixing $t = k+1$. With this choice, $\underline{\mathbf{T}}_{(k,k+1)}$ is simply shown as $\underline{\mathbf{T}}_{[k]}$.

Given $\underline{\mathbf{L}} \in \mathbb{R}^{I_1 \times I_2 \times I_3}$, define its 1D Fourier transform that is applied on all fibers by $\mathfrak{F}(\underline{\mathbf{L}}) \in \mathbb{C}^{I_1 \times I_2 \times I_3}$. The tubal nuclear norm is given by the average of the nuclear norm of all of the frontal slices of $\mathfrak{F}(\underline{\mathbf{L}})$, that is,

$$||\,\underline{\mathbf{L}}\,||_{\text{TNN}} = \frac{1}{I_3} \sum_{i_3=1}^{I_3} ||\mathfrak{F}(\underline{\mathbf{L}})_{i_3}||_* \,. \tag{9}$$

The proximity operator for the tubal nuclear norm is given by

$$\text{Prox}^{||\cdot||_{\text{TNN}}}_{\frac{\gamma_L}{\rho}}(\underline{\mathbf{L}}) = \underline{\mathbf{U}} * \mathfrak{F}^{-1}(\max\{\mathfrak{F}(\underline{\boldsymbol{\lambda}}) - \frac{\gamma_L}{\rho}, \underline{\mathbf{0}}\}) * \underline{\mathbf{V}}^T \;. \tag{10}$$

In [12], the optimization problem given at (3) is solved similarly to SNN, while only changing the rank relaxation into the tubal nuclear norm. This can be formulated as

$$\min_{\underline{\mathbf{L}},\underline{\mathbf{S}}} \left\{ \frac{1}{2} ||\,\underline{\mathbf{L}} + \underline{\mathbf{S}} - \underline{\mathbf{Y}}\,||_F^2 + \gamma_L ||\,\underline{\mathbf{L}}||_{\text{TNN}} + \gamma_S ||\,\underline{\mathbf{S}}\,||_1 \right\}. \tag{11}$$

Under the tensor incoherence condition (see [12]), the exact recovery of the true tensor $\underline{\mathbf{L}}$ is guaranteed for the noiseless case. This algorithm is named the tensor stable principal component pursuit (TSPCP). In [16], an additional constraint regarding the infinity norm of the low-rank tensor is added to the objective function such that the absolute values of $\underline{\mathbf{L}}$ are below a certain threshold and the outliers are captured at $\underline{\mathbf{S}}$ instead. This optimization problem can be shown as

$$\min_{\underline{\mathbf{L}},\underline{\mathbf{S}}} \left\{ \frac{1}{2} ||\,\underline{\mathbf{L}} + \underline{\mathbf{S}} - \underline{\mathbf{Y}}\,||_F^2 + \gamma_L ||\,\underline{\mathbf{L}}||_{\text{TNN}} + \gamma_S ||\,\underline{\mathbf{S}}\,||_1 \right\} \quad \text{s.t.} \quad ||\,\underline{\mathbf{L}}\,||_\infty \leq \alpha \,. \tag{12}$$

The constraint regarding the infinity norm is handled by clipping the maximum value of the absolute value of $\underline{\mathbf{L}}$ to α at each iteration of the optimization.

Only the low rankness in the third mode is incorporated in (12) and (11). The authors in [13] extended the analysis to all the modes for general N-dimensional tensors $\underline{\mathbf{L}} \in \mathbb{R}^{I_1 \times \cdots \times I_N}$, $\underline{\mathbf{S}} \in \mathbb{R}^{I_1 \times \cdots \times I_N}$, and $\underline{\mathbf{W}} \in \mathbb{R}^{I_1 \times \cdots \times I_N}$ using the mode (k,t) unfolding. According to Lemma 1 in [13], any tensor that has a low Tucker rank has a low orientation invariant average rank. This enables the direct application of two convex proxy methods, OITNN-O and OITNN-L, onto low Tucker rank applications using the orientation invariant tubal nuclear norm (OITNN). The OITNN is defined as

$$||\,\underline{\mathbf{L}}\,||_{\text{OITNN}} = \frac{1}{N} \sum_{n=1}^{N} ||\,\underline{\mathbf{L}}_{[n]}\,||_{\text{TNN}} \,. \tag{13}$$

The OITNN-O considers the low rankness in all orientations and solves the optimization problem that is defined as

$$\min_{\underline{\mathbf{L}},\underline{\mathbf{S}}} \left\{ \frac{1}{2} ||\,\underline{\mathbf{L}} + \underline{\mathbf{S}} - \underline{\mathbf{Y}}\,||_F^2 + \gamma_L ||\,\underline{\mathbf{L}}||_{\text{OITNN}} + \gamma_S ||\,\underline{\mathbf{S}}\,||_1 \right\} \quad \text{s.t.} \quad ||\,\underline{\mathbf{L}}\,||_\infty \leq \alpha \,. \tag{14}$$

The OITNN-L considers $\underline{\mathbf{L}}$ as the sum of N auxiliary tensors, which can have a low tubal rank in their respective mode. Assuming that an incoherence condition holds, this optimization problem is defined as

$$\min_{\underline{\mathbf{L}}^{(1)},\dots,\underline{\mathbf{L}}^{(N)},\underline{\mathbf{S}}} \left\{ \frac{1}{2} ||\sum_k \underline{\mathbf{L}}^{(k)} + \underline{\mathbf{S}} - \underline{\mathbf{Y}}\,||_F^2 + \frac{\gamma_L}{N} \sum_n ||\,\underline{\mathbf{L}}^{(n)}_{[n]}\,||_{\text{TNN}} + \gamma_S ||\,\underline{\mathbf{S}}\,||_1 \right\} \quad \text{s.t.} \quad ||\sum_n \underline{\mathbf{L}}^{(n)}\,||_\infty \leq \alpha \,. \tag{15}$$

The exact recovery of true $\underline{\mathbf{L}}$ is not guaranteed for the noiseless case when the infinity norm constraint is incorporated.

VI. Simulation

This section compares the denoising performance of the methods given in Table 1 through a Monte Carlo simulation. Here, we have generated two 3D tensors of size $\underline{\mathbf{L}} \in \mathbb{R}^{20 \times 20 \times 20}$ with unequal ranks and equal ranks. This is done by generating a core tensor of size $(10, 10, 10)$ and $(5, 10, 15)$ from a standard uniform distribution, multiplying it in each mode with unitary factor matrices, and finally taking the logarithm. The noise tensor is generated by taking the logarithm of tensor $\underline{\mathbf{M}} \in \mathbb{R}^{20 \times 20 \times 20}$ where each entry $m_{i_1 i_2 i_3}$

TABLE I
SUMMARY OF THE METHODS THAT ARE USED IN THIS PAPER.

	Constraints	Noise	Optimization problem
HOOI [17]	Ranks	WGN	-
tr-MLSVD [18]	Ranks	WGN	-
wSNN	Ranks	WGN + Sparse	(4) and (8)
SNN [9]	-	WGN + Sparse	(4) and (5)
TNN [19]	$\|\|\underline{\mathbf{L}}\|\|_\infty$	WGN + Sparse	(12)
OITNN-O [13]	$\|\|\underline{\mathbf{L}}\|\|_\infty$	WGN + Sparse	(14)
OITNN-L [13]	$\|\|\underline{\mathbf{L}}\|\|_\infty$	WGN + Sparse	(15)
TSPCP [12]	-	WGN + Sparse	(11)

follows the Rayleigh distribution with a scaling parameter of 1. The SNR of the problem is defined by

$$10\log_{10}\left(\frac{\mathbb{E}[\underline{\mathbf{L}}-\mathbb{E}[\underline{\mathbf{L}}]]^2}{\mathbb{E}[\underline{\mathbf{M}}-\mathbb{E}[\underline{\mathbf{M}}]]^2}\right). \tag{16}$$

We have scaled the variance of $\underline{\mathbf{L}}$ while fixing the scaling parameter of the noise such that SNRs of $\{-5, 0, 5, 10, 15, 20, 25, 30\}$ are obtained. The noisy tensor $\underline{\mathbf{Y}}$ is obtained by the summation of $\underline{\mathbf{L}}$ and $\underline{\mathbf{M}}$. The normalized error is used as a performance metric, which is defined as

$$20\log_{10}\frac{||\hat{\underline{\mathbf{L}}}-\underline{\mathbf{L}}||_F}{||\underline{\mathbf{L}}||_F}. \tag{17}$$

Ten numbers in the range $(1, 100)$ are traversed for optimization of the parameters γ_S and γ_L for OITNN-L, while the range $(1, 30)$ are traversed for the rest of the robust tensor decomposition methods. We fixed the value of ρ to 1 and set the maximum iteration number to 500. The true ranks are used for tr-MLSVD and HOOI, and the true $||\underline{\mathbf{L}}||_\infty$ is assigned to α for TNN, OITNN-O, and OITNN-L.

VII. RESULTS

The simulation defined in Section VI is repeated for 20 random initialization of the noise tensor and true tensor. The normalized error is calculated for various SNRs and plotted in Fig. 1. For each run of the algorithm, the best-performing tuning parameters γ_S and γ_L are selected to calculate the normalized error. For all SNRs, the wSNN performs better than the truncated multilinear singular value decomposition and HOOI. More improvement is found for low SNR scenarios. The best-performing method is OTINN_L for both ranks when the SNR is less than 20 dB. For SNRs greater than 20 dB, the wSNN performs better with a small improvement compared to HOOI.

VIII. DISCUSSION AND CONCLUSION

This paper compares low-rank tensor decomposition methods for despeckling applications. We have proposed a weighting scheme for SNN-based algorithms when the ranks are known and compared the results to robust tensor decomposition methods. All robust tensor decomposition algorithms outperform HOOI and tr-MLSVD for low SNRs because of the better noise model. We have observed that wSNN performs better than HOOI and tr-MLSVD for high SNR

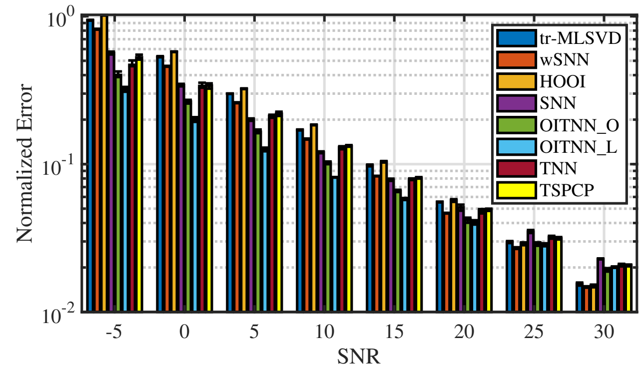

(a)

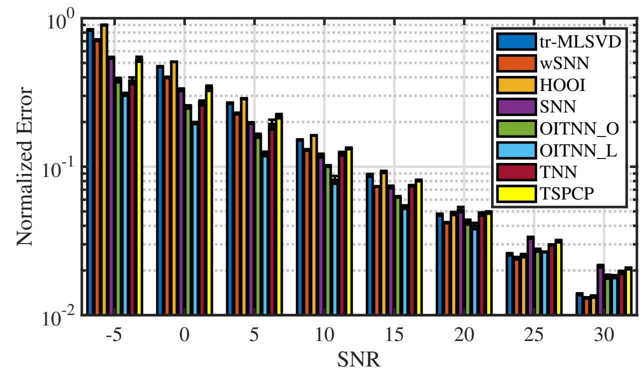

(b)

Fig. 1. The plot of the normalized error versus SNR for various low rank over a 20 Monte Carlo simulations. The plots with subscripts (a) and (b) represent the ranks $(10, 10, 10)$ and $(5, 10, 15)$, respectively.

scenarios. The weights of wSNN are arranged such that the highest singular values that correspond with the true rank are not updated during the proximity operator update. This resembles the tr-MLSVD, where the singular values with an index greater than the rank are truncated for denoising. Alongside this property, the sparsity constraint that is added to the formulation of wSNN results in a better recovery. For low SNR scenarios, wSNN performed worse than SNN. This is due to the corruption of the singular values with the noise subspace. The utilization of the proximity operator shown in (8) restricts the updating of singular values associated with the rank. Consequently, the denoising capabilities of wSNN are constrained by a diminished search space, thus contributing to its reduced performance under low SNR conditions.

Among the convex relaxations, TNN performs better than SNN for low SNRs. The algorithm proposed in [19] considers the low rankness in only one of the dimensions using the t-SVD framework. In our simulations, we generated a tensor with a low Tucker rank in all the dimensions. Hence, algorithms such as OITNN-L and OITNN-O that incorporate the low rankness in all the dimensions have performed better. Although OITNN-O is expected to perform worse when the tensor is lower-rank in some dimensions than others, we have not observed this in our simulation. OITNN-L is found to be the algorithm that performed the best for low SNR scenarios regardless of the ranks. The sparse outliers have minimal effect on the low-rank approximation for SNRs greater than 20 dB. This might be because, as the noise intensity decreases, the noise after the logarithmic transformation becomes closer to a Gaussian distribution, diminishing the impact of sparsity.

One of the limitations of this paper is the grid search on the low-rankness and sparsity-related tuning parameters γ_S and γ_L. We have defined the range such that a convex range of normalized mean squared error has been observed. By extending the grid search, a better comparison can be made among the convex low-rank approximation methods. This paper aims to understand the importance of sparsity constraint in denoising speckle noise. The HOOI and tr-MLSVD are better suited for denoising WGN. The fact that the robust low-rank approximation methods perform better than HOOI and tr-MLSVD proves the added benefit of the sparsity constraint. We compare the results of the SNN and TNN-based methods in a heuristic manner. A better approach for this comparison would be optimizing the tuning parameters using methods such as [20].

Another limitation of the paper is the need for a quantization analysis for the low-rank tensor $\underline{\mathbf{L}}$. During the simulation, we scaled the variance of $\underline{\mathbf{L}}$ to reach the predefined SNRs. In many despeckling applications, such as ultrasound, the input is 8-bit unsigned integers. An analysis that covers the effect of the quantization on the despeckling applications is left for future work, along with real-world applications. In addition, we have assumed that the rank of true tensor $\underline{\mathbf{L}}$ is known and defined the weighting parameter given at (7) according to this rank. The ranks of the system can be estimated using the outlier resistant rank estimation methods such as the one given in [21]. The algorithm could be modified such that the ranks are not known. In such a case, the higher singular values can be thresholded less using techniques such as [7]. Finally, non-linear transformations such as the log transformation might increase the rank of the tensor. In real-world applications with limited quantization, further analysis is required.

TNN and TSPCP are defined for 3D tensors that can be applied to speckle denoising applications where 2D non-local correlated patches are stacked to create the tensor. For applications like 4D ultrasound or MRI, orientation-insensitive TNN methods such as OITNN-O and OITNN-L could be used. SNN methods are directly applicable to any dimensional tensor. Hence, they can be immediately applied to a 4D speckle denoising application. In conclusion, we have reviewed various low-rank approximation methods for denoising speckle noise and found that incorporating the sparsity constraint is useful, especially for low SNR scenarios.

References

[1] N. Yahya, N. S. Kamel, and A. S. Malik, "Subspace-based technique for speckle noise reduction in sar images," *IEEE Transactions on Geoscience and Remote Sensing*, vol. 52, no. 10, pp. 6257–6271, 2014.

[2] J. Grabek and B. Cyganek, "Speckle noise filtering in side-scan sonar images based on the tucker tensor decomposition," *Sensors*, vol. 19, no. 13, 2019.

[3] O. V. Michailovich and A. Tannenbaum, "Despeckling of medical ultrasound images," *ieee transactions on ultrasonics, ferroelectrics, and frequency control*, vol. 53, no. 1, pp. 64–78, 2006.

[4] J. Bioucas-Dias and M. Figueiredo, "Multiplicative noise removal using variable splitting and constrained optimization," *Image Processing, IEEE Transactions on*, vol. 19, pp. 1720 – 1730, 08 2010.

[5] Y. Dong and T. Zeng, "A convex variational model for restoring blurred images with multiplicative noise," *SIAM Journal on Imaging Sciences*, vol. 6, no. 3, pp. 1598–1625, 2013.

[6] J. Fang, T. Mao, F. Bo, B. Hao, N. Zhang, S. Hu, W. Lu, and X. Wang, "An sar image-despeckling method based on hosvd using tensor patches," *Remote Sensing*, vol. 15, no. 12, p. 3118, 2023.

[7] S. V. M. Sagheer, S. N. George, and S. K. Kurien, "Despeckling of 3d ultrasound image using tensor low rank approximation," *Biomedical Signal Processing and Control*, vol. 54, p. 101595, 2019.

[8] D. Goldfarb and Z. T. Qin, "Robust low-rank tensor recovery: Models and algorithms," *SIAM Journal on Matrix Analysis and Applications*, vol. 35, pp. 225–253, jan 2014.

[9] Q. Gu, H. Gui, and J. Han, "Robust tensor decomposition with gross corruption," *Advances in Neural Information Processing Systems*, vol. 27, 2014.

[10] R. Tomioka and T. Suzuki, "Convex tensor decomposition via structured schatten norm regularization," *Advances in neural information processing systems*, vol. 26, 2013.

[11] C. Lu, J. Feng, Y. Chen, W. Liu, Z. Lin, and S. Yan, "Tensor robust principal component analysis with a new tensor nuclear norm," *IEEE transactions on pattern analysis and machine intelligence*, vol. 42, no. 4, pp. 925–938, 2019.

[12] W. Fang, D. Wei, and R. Zhang, "Stable tensor principal component pursuit: Error bounds and efficient algorithms," *Sensors*, vol. 19, no. 23, p. 5335, 2019.

[13] A. Wang, Q. Zhao, Z. Jin, C. Li, and G. Zhou, "Robust tensor decomposition via orientation invariant tubal nuclear norms," *Science China Technological Sciences*, vol. 65, no. 6, pp. 1300–1317, 2022.

[14] S. Gu, L. Zhang, W. Zuo, and X. Feng, "Weighted nuclear norm minimization with application to image denoising," in *Proceedings of the IEEE conference on computer vision and pattern recognition*, pp. 2862–2869, 2014.

[15] M. E. Kilmer, K. Braman, N. Hao, and R. C. Hoover, "Third-order tensors as operators on matrices: A theoretical and computational framework with applications in imaging," *SIAM Journal on Matrix Analysis and Applications*, vol. 34, no. 1, pp. 148–172, 2013.

[16] A. Wang, Z. Jin, and G. Tang, "Robust tensor decomposition via t-svd: Near-optimal statistical guarantee and scalable algorithms," *Signal Processing*, vol. 167, p. 107319, 2020.

[17] L. De Lathauwer, B. De Moor, and J. Vandewalle, "On the best rank-1 and rank-(r1 ,r2 ,. . .,rn) approximation of higher-order tensors," *SIAM Journal on Matrix Analysis and Applications*, vol. 21, no. 4, pp. 1324–1342, 2000.

[18] L. De Lathauwer, B. De Moor, and J. Vandewalle, "A multilinear singular value decomposition," *SIAM journal on Matrix Analysis and Applications*, vol. 21, no. 4, pp. 1253–1278, 2000.

[19] Z. Zhang, G. Ely, S. Aeron, N. Hao, and M. Kilmer, "Novel methods for multilinear data completion and de-noising based on tensor-svd," in *2014 IEEE Conference on Computer Vision and Pattern Recognition*, pp. 3842–3849, 2014.

[20] Q. Zhao, G. Zhou, L. Zhang, A. Cichocki, and S.-I. Amari, "Bayesian robust tensor factorization for incomplete multiway data," *IEEE transactions on neural networks and learning systems*, vol. 27, no. 4, pp. 736–748, 2015.

[21] T. Yokota, N. Lee, and A. Cichocki, "Robust multilinear tensor rank estimation using higher order singular value decomposition and information criteria," *IEEE Transactions on Signal Processing*, vol. 65, no. 5, pp. 1196–1206, 2016.